Group-IV and group-V substitutional impurities in cubic group-III nitrides

L. E. Ramos,[1] J. Furthmüller,[1] J. R. Leite,[2] L. M. R. Scolfaro,[2] and F. Bechstedt[1]
[1]*Institut für Festkörpertheorie und Theoretische Optik, Friedrich-Schiller-Universität, 07743 Jena, Germany*
[2]*Universidade de São Paulo, Instituto de Física, CP66318, 05315-970 São Paulo SP, Brazil*
(Received 4 December 2002; revised manuscript received 29 April 2003; published 29 August 2003)

We present *ab initio* pseudopotential plane-wave calculations for C, Si, Ge, P, As, and Sb on substitutional sites in cubic AlN and GaN for several charge states. The stability of these impurities, the geometry of the nearest neighbors, as well as the defect levels are studied in large supercells, reducing the impurity-impurity interaction and the alloying effect inherent the small supercells. Due to the large number of electrons in the supercell, higher charge states can be studied with less perturbation of the system. The trend of the defect levels and stability with respect to the atomic number of the impurity is analyzed in order to provide information about alternative dopants for the nitrides. Different growth and preparation conditions are considered. We estimate the partial concentrations of the incorporated impurities according to their charge states and versus the total amount of impurities available.

DOI: 10.1103/PhysRevB.68.085209 PACS number(s): 71.55.−i, 61.72.Vv

I. INTRODUCTION

Group-III nitrides crystallize usually in the hexagonal or wurtzite (*w*) phase.[1] However, the cubic (*c*) or zinc blende phase of these compounds offers in principle many advantages such as a high symmetry, lack of spontaneous-polarization effects, and it is more suitable to *p* doping.[2] Since the structural differences between the cubic and wurtzite phases refer only to the positions of the second neighbors, it is useful to compare the results obtained for the impurities in these two phases. The group-IV elements silicon and germanium have been traditionally used as dopant elements in order to achieve *n*-type conductivity in AlN and GaN.[3–7] Differently from silicon and germanium which have been applied in semiconductor technology for many years, carbon has been recently quoted to obtain *p*-type conductivity in *c*-GaN (Ref. 8) with some advantages with respect to Mg_{Ga}, since it can be incorporated in higher concentrations[9] than Mg and the activation energies are reduced in the case of the cubic phase.[10] Moreover, carbon is an unintentional impurity during the growth of group-III nitrides.[11–14]

On the other hand, group-V impurities have low solubility in nitrides and are often applied as surfactants.[2,15,16] When acting as surfactants, these impurities can modify significantly the properties of the growing surface without incorporating into the sample. By adding phosphorus during the growth of hexagonal GaN, one can induce the growth of layers of the cubic phase of the material.[15] The reconstruction properties of GaN surfaces are modified when a small amount of arsenic is added during the growth.[2] Antimony has been used as a surfactant in GaN surfaces[16] and other semiconductors[17] being incorporated in low concentrations. In addition to the residual character of the group-V impurities, they can be incorporated in the samples by means of ionic implantation[18] or under special growth conditions.[19] Recently the incorporation of P and As in GaN has been studied in order to provide preliminar information about GaNP and GaNAs alloys. Since GaP and GaAs have a lower lattice mismatch than InN in comparison to GaN, and a wide fundamental energy gap as well, the GaNP and GaNAs alloys could be alternative materials to perform similar to InGaN in some optoelectronic applications.[20,21]

The recent growth of zinc blende–phase crystals motivates a more detailed study of group-V impurities in group-III nitrides, in particular for AlN and GaN. One of the first theoretical investigations on group-IV and group-V impurities in group-III nitrides substitutionally on nitrogen sites (C, Si, Ge, P, As, and Sb) and cation sites (Si and Ge) was performed by Jenkins and Dow[22] applying the tight-binding method. Other works applied different methods for Si (Refs. 23,24) and Ge (Refs. 25,26) impurities in the zinc blende[27] and wurtzite phases of AlN and GaN. Park and Chadi conclude that Ge would be a good alternative to Si for doping AlGaN alloys[26] in accordance to experimental observation.[3,4] Mattila and Zunger studied the isovalent P and As impurities[28] as well as the pairs P-P and As-As in GaN (Ref. 29) motivated by the optical properties of GaNAs and GaNP alloys. Van de Walle and Neugebauer concluded that the single As impurity would be an obstacle to achieve *p*-type doping in GaN, and possibly would make *p* type impossible in GaNAs alloys as well.[30] Unless particular binding effects are involved, the incorporation of a given impurity on substitutional sites is usually favored to other sites.[31]

In this paper we investigate the incorporation of group-IV and group-V impurities on substitutional sites for zinc blende AlN and GaN, analysing the geometry of the nearest neighbors, the trend of the defect levels and ionization levels, and the formation energies. The C, Si, Ge, P, As, and Sb impurities are studied on the nitrogen and cation sites for several charge states and, when it is possible, a comparison to previous results in the literature is made. The paper is organized as follows. In Sec. II we describe the method applied to calculate the total energies, chemical potentials and defect levels. The results for each of the group-IV and group-V impurities are presented in Sec. III, and we summarize the results in Sec. IV.

II. METHOD

A. Total energies, *k*-point mesh, and geometry

The total energies for the systems with and without the impurity were calculated in the framework of the density

 ©2003 The American Physical Society

TABLE I. Orthornormal sets of basis used to project the displacement vectors of first- (1NN) and second- (2NN) nearest neighbors.

	1NN		2NN		
$\mathbf{b_{00}}$	$\frac{1}{\sqrt{3}}(1,1,1)$	$\mathbf{b_{0j}}$	$\frac{1}{\sqrt{2}}(0,1,1)$	$\frac{1}{\sqrt{2}}(1,1,0)$	$\frac{1}{\sqrt{2}}(1,0,1)$
$\mathbf{p_{00}}$	$\frac{1}{\sqrt{6}}(-1,-1,2)$	$\mathbf{p_{0j}}$	$\frac{1}{\sqrt{2}}(0,1,-1)$	$\frac{1}{\sqrt{2}}(1,-1,0)$	$\frac{1}{\sqrt{2}}(1,0,-1)$
$\mathbf{n_{00}}$	$\frac{1}{\sqrt{2}}(1,-1,0)$	$\mathbf{n_{0j}}$	$(1,0,0)$	$(0,0,1)$	$(0,1,0)$
$\mathbf{b_{10}}$	$\frac{1}{\sqrt{3}}(-1,1,-1)$	$\mathbf{b_{1j}}$	$\frac{1}{\sqrt{2}}(0,1,-1)$	$\frac{1}{\sqrt{2}}(-1,1,0)$	$\frac{1}{\sqrt{2}}(-1,0,-1)$
$\mathbf{p_{10}}$	$\frac{1}{\sqrt{6}}(1,-1,-2)$	$\mathbf{p_{1j}}$	$\frac{1}{\sqrt{2}}(0,1,1)$	$\frac{1}{\sqrt{2}}(-1,-1,0)$	$\frac{1}{\sqrt{2}}(-1,0,1)$
$\mathbf{n_{10}}$	$\frac{1}{\sqrt{2}}(-1,-1,0)$	$\mathbf{n_{1j}}$	$(-1,0,0)$	$(0,0,-1)$	$(0,1,0)$
$\mathbf{b_{20}}$	$\frac{1}{\sqrt{3}}(-1,-1,1)$	$\mathbf{b_{2j}}$	$\frac{1}{\sqrt{2}}(0,-1,1)$	$\frac{1}{\sqrt{2}}(-1,-1,0)$	$\frac{1}{\sqrt{2}}(-1,0,1)$
$\mathbf{p_{20}}$	$\frac{1}{\sqrt{6}}(1,1,2)$	$\mathbf{p_{2j}}$	$\frac{1}{\sqrt{2}}(0,-1,-1)$	$\frac{1}{\sqrt{2}}(-1,1,0)$	$\frac{1}{\sqrt{2}}(-1,0,-1)$
$\mathbf{n_{20}}$	$\frac{1}{\sqrt{2}}(-1,1,0)$	$\mathbf{n_{2j}}$	$(-1,0,0)$	$(0,0,1)$	$(0,-1,0)$
$\mathbf{b_{30}}$	$\frac{1}{\sqrt{3}}(1,-1,-1)$	$\mathbf{b_{3j}}$	$\frac{1}{\sqrt{2}}(0,-1,-1)$	$\frac{1}{\sqrt{2}}(1,-1,0)$	$\frac{1}{\sqrt{2}}(1,0,-1)$
$\mathbf{p_{30}}$	$\frac{1}{\sqrt{6}}(-1,1,-2)$	$\mathbf{p_{3j}}$	$\frac{1}{\sqrt{2}}(0,-1,1)$	$\frac{1}{\sqrt{2}}(1,1,0)$	$\frac{1}{\sqrt{2}}(1,0,1)$
$\mathbf{n_{30}}$	$\frac{1}{\sqrt{2}}(1,1,0)$	$\mathbf{n_{3j}}$	$(1,0,0)$	$(0,0,-1)$	$(0,-1,0)$

functional theory (DFT)[32] and local density approximation (LDA).[33] To describe the exchange and correlation energy per electron, we applied the parametrization of Perdew and Zunger[34] for the quantum Monte Carlo calculations of Ceperley and Alder.[35] The Ga $3d$ electrons are included as valence electrons, whereas the Sb $4d$, As $3d$, and Ge $3d$ electrons are frozen in the atomic core. The interaction between the atomic cores and valence electrons is treated by means of ultrasoft Vanderbilt pseudopotentials[36] implemented in the Vienna *ab initio* Simulation Package.[37] The ultrasoft pseudopotentials allow a significant reduction of the cutoff energy up to 15.4 Ry for Al, 17.7 Ry for Ga, 14.9 Ry for N, 18.8 Ry for P, 15.4 Ry for As, 12.7 Ry for Sb, 14.8 Ry for C, 12.8 Ry for Si, and 12.3 Ry for Ge. The Kohn-Sham (KS) equations are solved by the method of residual minimization band by band and the KS eigenvalues are interpreted as the electronic levels of the bulk material as well as the impurity levels. To model the bulk material with the impurity atom, we applied 216-atom simple-cubic supercells which assure we are far beyond the alloy regime. In Ref. 38, we studied the influence of the supercell size in several electronic properties related to C_N. The impurity-impurity interaction is inherent the use of the supercell method and affects the total energies. The large number of electrons in the 216-atom supercells allows us to consider the relevant charge states for the impurities changing less than 1% of the total number of electrons. This represents an advantage with respect to the calculations reported in the literature, where the number of atoms is usually not larger than 72. The occupation of the electronic states followed the zeroth order Methfessel-Paxton method with $\sigma = 0.1$ eV, which corresponds to a Gaussian smearing.[39]

The geometry of the fully relaxed atomic positions with respect to the ideal zinc blende structure was determined for the first-nearest (1NN) and second-nearest (2NN) neighbors. To describe completely the geometry of the neighboring atoms, one needs in principle sixteen sets of orthonormal basis ($\mathbf{b_{ij}}$, $\mathbf{p_{ij}}$, $\mathbf{n_{ij}}$) centered at each particular neighbor to project their displacement vectors on these sets. For the sets pre-

sented in Table I, the index $i=0,1,2,3$ with $j=0$ refers to the four first-nearest neighbors and the index $j=1,2,3$ refers to the respective second-nearest neighbors. In the basis sets corresponding to the first-nearest neighbors, $\mathbf{b_{i0}}$ are the breathing-mode vectors connecting the impurity to the neighbor, $\mathbf{p_{i0}}$ are the pairing-mode vectors, and $\mathbf{n_{i0}}$ are vectors perpendicular to the latter ones.[40] For the twelve second-nearest neighbors to the impurity, we apply different basis sets. In these basis sets, $\mathbf{b_{ij}}$ are the breathing-mode vectors as before, $\mathbf{p_{ij}}$ are vectors pointing to third neighbors lying on the same plane as the impurity, and the corresponding vectors $\mathbf{n_{ij}}$ are perpendicular to the latter ones. The sixteen basis sets allow one to describe the geometry of the neighbors to an atomic site, including the case of lowering of the local symmetry, when a so-called Jahn-Teller distortion occurs.[31] For the impurities considered here, we found no indication for a Jahn-Teller distortion, therefore four basis sets, one for the first neighbor and three for its corresponding three second neighbors distinct from the impurity, are sufficient to describe the geometry changes of the neighboring atoms. Moreover, the displacements of the nearest neighbors along the vectors $\mathbf{p_{ij}}$ (first and second neighbors) and $\mathbf{n_{i0}}$ (first neighbors) are found to be negligible or zero for the impurities considered.

B. Formation energies and chemical potentials

The stability of the C, Si, Ge, P, As, and Sb impurities is determined by their formation energies $\Omega_f(X\mathrm{N}{:}Z^q_{\mathrm{N},X},E_\mathrm{F}) = E_{\mathrm{tot}}(X\mathrm{N}{:}Z^{\,q}_{\mathrm{N},X}) - E^{\mathrm{ideal}}_{\mathrm{tot}}(X\mathrm{N}) + \mu(\mathrm{N},X) - \mu(Z) + qE_\mathrm{F}$, where X is the cation (Al or Ga), Z is the impurity atom (C, Si, Ge, P, As, and Sb) in its charge state q incorporated on a N or cation site (N, X), $E^{\mathrm{ideal}}_{\mathrm{tot}}(X\mathrm{N})$ is the total energy corresponding to the bulk, the μ's are the chemical potentials under given preparation conditions, and E_F is the chemical potential of the electron reservoir or Fermi level. E_F is usually written in terms of a reduced Fermi level ε_F, which varies from zero to the fundamental gap E_g of the host compound, and the energetical position of the valence band maximum (VBM) E_V, by $E_F=E_V+\varepsilon_F$. Unless the doping conditions are mentioned explicitly, we consider optimal formation energies in the following, i.e., N-rich (cation-rich) conditions for impurities on the cation (nitrogen) sites and p-type (n-type) doping level for positively (negatively) charged impurities. Due to the possibility of finding defect levels close to the conduction band minimum (CBM) $E_C = E_V+E_g$, we applied the DFT-LDA fundamental gaps ($E_g=3.29$ eV for AlN and 2.03 eV for GaN using the above described DFT-LDA) for the range of variation of ε_F. To determine the absolute position of E_V for the supercells with an impurity in the charge state q, we compare the shift of the electrostatic potential along one of the Cartesian axes for a supercell containing the impurity with respect to the corresponding bulk supercell.[41] Since, we found that this potential varies less than 50 meV with respect to q, we use the shift energy corresponding to $q=0$ to calculate the optimal formation energies of charge states and the ionization levels. The plain value of E_V from bulk gives already a good approximation in most of the studied cases. The chemical potentials of N and X are linearly dependent on each other by $\mu(X\mathrm{N}_{\mathrm{bulk}})=\mu(X)+\mu(\mathrm{N})$ in accordance to the mass action law,[42] where $\mu(X\mathrm{N}_{\mathrm{bulk}})$ is the chemical potential of the bulk compound XN (-16.40 eV for AlN and -13.94 eV for GaN). In thermodynamic equilibrium, the chemical potentials of the atomic species may differ from their corresponding bulk reservoirs in such a way that it is convenient to define variations $\Delta\mu=\mu-\mu_{\mathrm{bulk}}$. The upper limit of $\Delta\mu$ is zero for a given species and describes preparation conditions rich in this species. To determine the lower limit for the variation of the chemical potentials, we use the experimental heats of formation $\Delta H_f=3.28$ eV for AlN and 1.28 eV for GaN (Ref. 43) and the relation $-\Delta H_f(X\mathrm{N})=\Delta\mu(X)+\Delta\mu(\mathrm{N})$. This choice of experimental values for ΔH_f avoids the explicit determination of $\mu(\mathrm{N}_{\mathrm{bulk}})$ by means of the N_2 molecule. The determination of the cohesive energy of N_2 would require a much harder pseudopotential than the one used in our calculations. In addition to this, it is convenient to describe the preparation conditions by choosing as variable the nitrogen chemical potential $\mu(\mathrm{N})=\mu(X\mathrm{N}_{\mathrm{bulk}})-\mu(X_{\mathrm{bulk}})+\Delta H_f(X\mathrm{N})+\Delta\mu(\mathrm{N})$. N-rich preparation conditions correspond to $\Delta\mu(\mathrm{N})=0$ and X-rich preparation conditions to $\Delta\mu(\mathrm{N})=-\Delta H_f(X\mathrm{N})$.

The actual chemical potentials of the atomic species during the growth are usually unknown, since the source for the atomic species are complex gases and the whole process consists in several chemical reactions. In order to be consistent, one has to calculate these quantities using the same theoretical scheme as the one applied to calculate the total energies. The chemical potentials for the group-IV impurities C, Si, and Ge were obtained from DFT-LDA calculations for the diamond structure of these compounds: $\mu(\mathrm{C}_{\mathrm{bulk}})=-10.15$ eV, $\mu(\mathrm{Si}_{\mathrm{bulk}})=-5.92$ eV, and $\mu(\mathrm{Ge}_{\mathrm{bulk}})=-5.15$ eV. The group-V atomic species have the rhombohedral $A7$ as a common structure among many other polymorphs whose geometries can be more complex.[44] For that reason, to evaluate their bulk chemical potentials we only considered a simple-cubic structure. Using DFT-LDA and 20 **k** points in the irreducible wedge of the Brillouin zone one obtains $\mu(\mathrm{P}_{\mathrm{bulk}})=-5.91$ eV, $\mu(\mathrm{As}_{\mathrm{bulk}})=-5.18$ eV, and $\mu(\mathrm{Sb}_{\mathrm{bulk}})=-4.65$ eV. The chemical potentials determined by DFT-LDA using the geometry of the $A7$ structure optimized by other authors[44–46] give rise to slightly lower values by 0.1 -0.2 eV. The pseudopotentials for Al and Ga we use are the same as the ones described in Ref. 47 where the chemical potentials $\mu(\mathrm{Al}_{\mathrm{bulk}})=-4.19$ eV and $\mu(\mathrm{Ga}_{\mathrm{bulk}})=-3.58$ eV were calculated assuming a fcc structure.

C. Kohn-Sham defect levels, ionization levels, and relaxation energies

Defect levels are usually characterized by KS defect levels (single-particle picture) or by means of ionization levels calculated in the framework of the ΔSCF (delta self-consistent field) method. The KS eigenvalues associated to the defect states do not account for the excitation aspect inherent the ionization on a recharging of the defect. The ionization levels provide a more rigorous information about the defect levels, since they are calculated by differences between the total energies of the systems in certain charge

TABLE II. Displacements of the nearest neighbors 1NN and 2NN ($\Delta\mathbf{d}1,2$ in % of the bond length), lattice relaxation energy ΔE, optimal formation energy for the defect Ω_f (N-rich [cation-rich] for $C_{Al,Ga}$ [C_N] and *p*-type [*n*-type] for neutral and positively [negatively] ionized), KS defect levels ε_{KS} with respect to the VBM, and ionization levels $\varepsilon(q+1/q)$ for C in AlN and GaN.

Impurity		$\Delta\mathbf{d}1$	$\Delta\mathbf{d}2$		ΔE	Ω_f	ε_{KS}	$\varepsilon(q+1/q)$
		$\mathbf{b_{0j}}$	$\mathbf{b_{ij}}$	$\mathbf{n_{ij}}$	(eV)	(eV)	(eV)	(eV)
AlN	C_N^{3-}	−0.13	1.88	0.24	0.25	−0.28	3.29	3.27
	C_N^{2-}	−0.13	1.90	0.23	0.26	−0.26	3.29	3.25
	C_N^{1-}	−0.13	1.91	0.23	0.28	−0.21	1.02	0.80
	C_N^{0}	2.51	1.41	0.04	0.12	2.28	0.52	0.39
	C_N^{1+}	4.34	1.19	−0.14	0.24	1.89	0.25	0.19
	C_N^{2+}	5.28	1.09	−0.26	0.34	1.70	0.15	0.09
	C_N^{3+}	5.75	1.06	−0.32	0.38	1.61	0.10	
	C_{Al}^{2-}	−15.97	−2.59	1.45	2.12	4.05	3.20	3.20
	C_{Al}^{1-}	−15.99	−2.61	1.50	2.15	4.15	3.21	3.19
	C_{Al}^{0}	−16.00	−2.62	1.53	2.20	4.26	3.22	3.17
GaN	C_N^{1-}	−1.31	1.36	0.18	0.23	0.82	0.26	0.26
	C_N^{0}	−0.38	1.14	0.11	0.07	2.59	0.16	0.16
	C_N^{1+}	0.16	1.04	0.06	0.04	2.43	0.12	0.11
	C_N^{2+}	0.48	0.99	0.02	0.04	2.32	0.09	0.07
	C_N^{3+}	0.74	0.97	0.00	0.04	2.25	0.07	
	C_{Ga}^{1-}	−18.87	−3.81	1.03	2.79	3.63	1.87	1.90
	C_{Ga}^{0}	−18.82	−3.81	1.10	3.01	3.76	1.87	1.85

TABLE III. Displacements of the nearest neighbors 1NN and 2NN ($\Delta\mathbf{d}1,2$ in % of the bond length), lattice relaxation energy ΔE, optimal formation energy for the defect Ω_f (N-rich [cation-rich] for $Si_{Al,Ga}$ [Si_N] and *p*-type [*n*-type] for neutral and positively [negatively] ionized), KS defect levels ε_{KS} with respect to the VBM, and ionization levels $\varepsilon(q+1/q)$ for Si in AlN and GaN.

Impurity		$\Delta\mathbf{d}1$	$\Delta\mathbf{d}2$		ΔE	Ω_f	ε_{KS}	$\varepsilon(q+1/q)$
		$\mathbf{b_{0j}}$	$\mathbf{b_{ij}}$	$\mathbf{n_{ij}}$	(eV)	(eV)	(eV)	(eV)
AlN	Si_N^{2-}	16.56	6.99	0.40	5.66	4.56	3.26	3.25
	Si_N^{1-}	16.00	7.00	0.41	5.65	4.60	2.21	2.07
	Si_N^{0}	18.13	5.94	0.20	6.45	5.83	1.82	1.67
	Si_N^{1+}	20.55	4.97	−0.02	7.52	4.16	1.47	1.34
	Si_N^{2+}	23.21	4.09	−0.28	8.58	2.82	1.20	1.08
	Si_N^{3+}	26.12	3.29	−0.51	9.50	1.74	0.99	0.89
	Si_N^{4+}	29.22	2.41	−0.76	10.28	0.85	0.85	
	Si_{Al}^{3-}	−5.59	0.15	−0.80	0.62	−2.19	3.18	3.19
	Si_{Al}^{2-}	−5.64	0.16	−0.82	0.65	−2.08	3.19	3.18
	Si_{Al}^{1-}	−5.68	0.18	−0.84	0.68	−1.97	3.20	3.18
	Si_{Al}^{0}	−5.72	0.20	−0.86	0.72	−1.86	3.20	3.16
GaN	Si_N^{1-}	12.65	5.87	0.01	3.59	3.80	1.19	1.11
	Si_N^{0}	14.64	5.11	−0.14	4.00	4.71	0.94	0.85
	Si_N^{1+}	16.38	4.40	−0.30	4.46	3.86	0.72	0.64
	Si_N^{2+}	17.74	3.73	−0.46	4.83	3.22	0.55	0.47
	Si_N^{3+}	18.82	3.22	−0.59	5.10	2.74	0.42	0.35
	Si_N^{4+}	19.65	2.82	−0.72	5.30	2.39	0.34	
	Si_{Ga}^{1-}	−8.07	−0.52	−0.69	1.08	−2.20	1.93	1.96
	Si_{Ga}^{0}	−8.06	−0.50	−0.70	1.10	−2.14	1.94	1.91

states. The position of the KS defect levels in the fundamental gap is determined by the alignment procedure, whereas the acceptorlike ionization levels[31] are calculated by $\varepsilon(q+1/q)=E_{tot}(X\mathrm{N}:Z^{q}_{\mathrm{N},X})-E_{tot}(X\mathrm{N}:Z^{q+1}_{\mathrm{N},X})-E_V$, where Z=C, Si, Ge, P, As, and Sb are the impurity atoms in a given charge state q, X=Al or Ga, and E_V is the aligned top of valence band. All the ionization energies refer to the VBM, independent of the eventual acceptor or donor character. Corrections due to the band gap underestimated in DFT-LDA are not taken into account in our results. In order to do this, different procedures are suggested. The simplest procedure is to increase the fundamental gaps according to the experimental or quasiparticle values.[48] Another procedure is to represent all ionization levels which include negatively charged states with respect to the CBM and the ones which include positively charged states with respect to the VBM.[49] Then experimental values or theoretical values including quasiparticle corrections for the bandgap are applied. As a consequence, the ionization levels are shifted with respect to the CBM. In a third procedure, the defect levels in the gap are shifted by a fraction of the quasiparticle gap opening proportional to the overlap of their wave functions with the conduction-band states.[50]

The incorporation of the impurity on a subtitutional site implies some displacements of the atoms on the neighboring sites. A comparison between the covalent radius of the impurity[51] and the covalent radius of the replaced atom in the host crystal allows to preview the general trend for the relaxation of the neighboring atoms. The difference between the total energies of the system where all the atoms are at ideal zinc blende sites and the system with the relaxed atomic positions is the lattice relaxation energy $\Delta E(Z^{q}_{\mathrm{N},X})=E^{ideal}_{tot}(X\mathrm{N}:Z^{q}_{\mathrm{N},X})-E_{tot}(X\mathrm{N}:Z^{q}_{\mathrm{N},X})$. Together with the displacements given in percentage of the bond length d (d=1.879 Å for AlN and d=1.931 Å for GaN) and formation energies, the relaxation energy provides information about the strength of the atomic relaxation around the impurity.

III. RESULTS

A. Carbon

The atomic displacements of the first- and second-nearest neighbors, the relaxation energy, the optimal formation energy, Kohn-Sham defect levels, and ionization levels for the C impurity are listed in Table II. C on the Al site produces an inward breathing-mode relaxation for the first and second neighbors. On the N site of AlN, the first neighbors of C show very short inward displacements for the negatively charged states, including the isovalent case $q=1-$. For the neutral and positively charged states, an outward relaxation occurs. The relaxation energies are lower for C_N than for C_{Al} in AlN. The optimal formation energies are lower for C_N than for C_{Al} in AlN. C_{Al} induces the shallow donor level $\varepsilon(1+/0)$, whereas C_N induces the deep acceptor level $\varepsilon(0/1$

TABLE IV. Displacements of the nearest neighbors 1NN and 2NN ($\Delta\mathbf{d}1,2$ in % of the bond length), lattice relaxation energy ΔE, optimal formation energy for the defect Ω_f (N-rich [cation-rich] for $Ge_{Al,Ga}$ [Ge_N] and *p*-type [*n*-type] for neutral and positively [negatively] ionized), KS defect levels ε_{KS} with respect to the VBM, and ionization levels $\varepsilon(q+1/q)$ for Ge in AlN and GaN.

Impurity		$\Delta\mathbf{d}1$	$\Delta\mathbf{d}2$		ΔE	Ω_f	ε_{KS}	$\varepsilon(q+1/q)$
		$\mathbf{b_{0j}}$	$\mathbf{b_{ij}}$	$\mathbf{n_{ij}}$	(eV)	(eV)	(eV)	(eV)
AlN	Ge_N^{2-}	16.70	7.11	0.44	6.04	4.47	3.26	3.24
	Ge_N^{1-}	16.50	7.12	0.47	6.00	4.51	2.24	2.11
	Ge_N^{0}	18.69	6.08	0.25	6.86	5.70	1.87	1.73
	Ge_N^{1+}	21.23	5.15	0.02	7.99	3.97	1.54	1.41
	Ge_N^{2+}	23.99	4.24	−0.23	9.12	2.56	1.28	1.18
	Ge_N^{3+}	27.08	3.39	−0.47	10.13	1.38	1.09	1.00
	Ge_N^{4+}	30.49	2.44	−0.72	11.01	0.38	0.97	
	Ge_{Al}^{3-}	−0.69	1.31	−0.78	0.19	−0.04	3.19	3.20
	Ge_{Al}^{2-}	−0.73	1.33	−0.79	0.20	0.06	3.19	3.19
	Ge_{Al}^{1-}	−0.77	1.35	−0.80	0.22	0.17	3.20	3.18
	Ge_{Al}^{0}	−0.81	1.37	−0.81	0.24	0.28	3.21	3.16
GaN	Ge_N^{1-}	13.64	6.08	0.03	4.09	3.87	1.28	1.20
	Ge_N^{0}	15.61	5.35	−0.13	4.58	4.70	1.03	0.93
	Ge_N^{1+}	17.30	4.55	−0.28	5.10	3.76	0.80	0.72
	Ge_N^{2+}	18.79	3.81	−0.48	5.54	3.04	0.62	0.54
	Ge_N^{3+}	20.07	3.24	−0.62	5.87	2.50	0.48	0.41
	Ge_N^{4+}	21.22	2.74	−0.77	6.11	2.09	0.39	
	Ge_{Ga}^{1-}	−2.86	0.89	−0.67	0.29	−0.20	1.93	1.96
	Ge_{Ga}^{0}	−2.93	0.90	−0.69	0.32	−0.13	1.93	1.91

−) and the shallow donor $\varepsilon(1-/2-)$. When incorporating in GaN on the Ga site, C requires inward relaxations of the first neighbors and second neighbors. For C occupying the N site, the displacements of the first and second neighbors are inward or outward according to the charge state. The relaxation energies for C_N are extremely low, showing that C replaces N in GaN with minimum perturbation of the lattice. C on the N site induces the shallow acceptor level $\varepsilon(0/1-)$. The position of the level calculated with respect to the VBM is in good agreement with the experimental value 215 meV reported by As and Köhler.[8] On the Ga site, C impurity has both formation and relaxation energies higher than for C_N and introduces the shallow donor level $\varepsilon(1+/0)$.

B. Silicon

In Table III we show the effect of the incorporation of Si in the relaxed atomic positions of the nearest neighbors and the corresponding optimal formation energies and defects levels. On the Al site, Si induces an inward relaxation of about 6% for the first neighbors and slight outward relaxations for the second neighbors. The relaxation energies for Si_{Al} are low, but higher than the one calculated by Bogusławski and Bernholc for the Si impurity in the wurtzite structure of AlN.[25] The calculated ionization levels indicate that Si_{Al} introduces the shallow donor level $\varepsilon(1+/0)$ in the fundamental gap. On the other hand, on the N site we calculate the deep donor level $\varepsilon(0/1-)$ and the shallow donor level $\varepsilon(1-/2-)$. Under optimal preparation conditions, the formation energies for Si_{Al} are negative. Considering the trend of formation energies towards lower values, we conclude that Si_{Al} is very likely to occur. Van de Walle and co-workers calculated formation energies even more negative for Si_{Al}^0 than -1.86 eV under *p*-type preparation conditions.[24] This difference may be due to the small 32-atom supercells used in their calculation, which increase the impurity-impurity interaction in the supercell method. The absence of defect levels in the fundamental gap was predicted by Jenkins and Dow[22] for Si_{Al} in the wurtzite phase of AlN. On the N site of *c*-AlN, Si induces an outward breathing-mode relaxation in the first and second neighbors, in accordance to results for the wurtzite phase in Ref. 25. The relaxation energies are higher for Si_{Al} in comparison to Si_N. Formation energies for Si on this site are relatively high, decreasing for higher charge states *q*. On the Ga site in GaN, Si induces inward breathing-mode relaxations for both first and second neighbors in order to reach the energy minimum. The relaxation energies for Si_{Ga} are slightly higher than for Si_{Al}, though the lattice constant of GaN is larger than the AlN one. For Si_{Ga} in *w*-GaN Bogusławski and Bernholc predict smaller inward relaxations of 5.6% for the first neighbors and lower relaxation energies of 0.65 eV.[25] The ionization levels indicate that Si_{Ga} introduces a shallow donor level $\varepsilon(1+/0)$ in the fundamental gap, in accordance to the results in Ref. 25 in which effective-mass levels were predicted. Neugebauer and Van de Walle[23,24] also predicted a donor level at 0.1 eV below the bottom of the conduction band. Götz and co-workers measured a donor level located 22 meV below the CBM in *w*-GaN:Si.[5] The level corresponding to the excitonic transition measured in *c*-GaN:Si is about 40 meV below the CBM according to As and co-workers.[7] Likewise Si_{Al}, the formation energies calculated for Si_{Ga} are negative and agree with those obtained by Van de Walle and co-workers[23,24] for the neutral charge state. The first and second neighbors of Si on the N site experience outward relaxations in GaN. The acceptor level $\varepsilon(0/1-)$, introduced by Si_N in GaN, lies close to the midgap and is followed by the corresponding KS defect levels. The formation energies of Si_N in GaN are comparable to the ones in AlN.

C. Germanium

The main information about the geometry and stability of a Ge impurity is given in Table IV. We found a remarkable difference between Si_{Al} and Ge_{Al} concerning the inward displacements of the first neighbors. The relaxation energies are low, showing that Ge replaces Al with a minimum perturbation of the lattice. Our results for the lattice relaxation differ considerably from the ones obtained by Bogusławski and Bernholc[25] for the Ge in wurtzite AlN, where the 1NN atoms are displaced by 17% of the bulk bond length and the relaxation energy is 0.9 eV. Concerning the stability, we calculate low formation energies for the neutral and negatively charged states. Taking into account the trend and values of the optimal formation energies, one may conclude that Si_{Al} is

TABLE V. Displacements of the nearest neighbors 1NN and 2NN ($\Delta\mathbf{d}1,2$ in % of the bond length), lattice relaxation energy ΔE, optimal formation energy for the defect Ω_f (N-rich [cation-rich] for $P_{Al,Ga}$ [P_N] and *p*-type [*n*-type] for neutral and positively [negatively] ionized), KS defect levels ε_{KS} with respect to the VBM, and ionization levels $\varepsilon(q+1/q)$ for P in AlN and GaN.

Impurity		$\Delta\mathbf{d}1$	$\Delta\mathbf{d}2$		ΔE	Ω_f	ε_{KS}	$\varepsilon(q+1/q)$
		$\mathbf{b_{0j}}$	$\mathbf{b_{ij}}$	$\mathbf{n_{ij}}$	(eV)	(eV)	(eV)	(eV)
	P_N^{2-}	15.84	4.81	0.14	5.16	1.23	3.24	3.27
	P_N^{1-}	15.74	4.82	0.16	5.18	1.25	3.25	3.23
	P_N^{0}	15.53	4.83	0.20	5.20	1.31	0.78	0.68
	P_N^{1+}	17.60	4.22	0.00	5.74	0.63	0.49	0.43
	P_N^{2+}	19.18	3.78	−0.20	6.07	0.21	0.33	0.28
AlN	P_N^{3+}	20.34	3.54	−0.34	6.30	−0.07	0.23	0.19
	P_N^{4+}	21.11	3.37	−0.44	6.45	−0.26	0.19	
	P_{Al}^{3-}	−9.35	0.81	−1.66	1.37	0.94	3.10	3.12
	P_{Al}^{2-}	−9.44	0.85	−1.71	1.46	1.12	3.10	3.12
	P_{Al}^{1-}	−9.59	0.90	−1.76	1.57	1.29	3.11	3.11
	P_{Al}^{0}	−9.68	0.94	−1.81	1.69	1.48	3.12	3.10
	P_{Al}^{1+}	−9.81	1.00	−1.87	1.85	−1.62	3.13	3.08
	P_N^{0}	13.29	4.17	−0.03	3.46	1.16	0.22	0.25
	P_N^{1+}	14.02	3.95	−0.11	3.55	0.91	0.18	0.19
	P_N^{2+}	14.44	3.84	−0.16	3.62	0.72	0.15	0.15
	P_N^{3+}	14.72	3.74	−0.20	3.66	0.57	0.13	0.11
GaN	P_N^{4+}	14.93	3.67	−0.23	3.71	0.46	0.11	
	P_{Ga}^{0}	−12.04	0.39	−1.50	1.82	0.62	1.87	1.90
	P_{Ga}^{1+}	−12.10	0.38	−1.54	2.10	−1.28	1.87	1.84

TABLE VI. Displacements of the nearest neighbors 1NN and 2NN ($\Delta\mathbf{d}1,2$ in % of the bond length), lattice relaxation energy ΔE, optimal formation energy for the defect Ω_f (N-rich [cation-rich] for $As_{Al,Ga}$ [As_N] and *p*-type [*n*-type] for neutral and positively [negatively] ionized), KS defect levels ε_{KS} with respect to the VBM, and ionization levels $\varepsilon(q+1/q)$ for As in AlN and GaN.

Impurity		$\Delta\mathbf{d}1$	$\Delta\mathbf{d}2$		ΔE	Ω_f	ε_{KS}	$\varepsilon(q+1/q)$
		$\mathbf{b_{0j}}$	$\mathbf{b_{ij}}$	$\mathbf{n_{ij}}$	(eV)	(eV)	(eV)	(eV)
	As_N^{2-}	18.50	5.65	0.19	7.22	2.24	3.22	3.26
	As_N^{1-}	18.32	5.65	0.22	7.20	2.27	3.24	3.22
	As_N^{0}	18.05	5.65	0.27	7.17	2.34	1.02	0.91
	As_N^{1+}	20.25	4.87	0.04	7.93	1.43	0.72	0.63
	As_N^{2+}	22.29	4.32	−0.17	8.45	0.80	0.51	0.45
	As_N^{3+}	23.98	3.82	−0.37	8.82	0.34	0.38	0.25
AlN	As_N^{4+}	25.42	3.47	−0.52	9.18	0.09	0.30	
	As_{Al}^{0}	1.55	2.60	−1.23	0.45	3.51	3.21	3.19
	As_{Al}^{1+}	2.19	2.70	−1.14	0.51	0.33	3.13	3.29
	As_{Al}^{2+}	−2.79	2.68	−1.80	1.14	−2.97	0.04	0.08
	As_{Al}^{3+}	−2.80	2.58	−1.78	1.07	−3.05	0.03	0.04
	As_{Al}^{4+}	−2.81	2.50	−1.75	1.01	−3.08	0.01	
	As_N^{1-}	15.95	4.93	−0.07	5.36	1.96	2.02	1.99
	As_N^{0}	15.85	4.92	−0.05	5.33	1.99	0.27	0.26
	As_N^{1+}	16.82	4.56	−0.17	5.51	1.73	0.16	0.16
GaN	As_N^{2+}	17.35	4.28	−0.27	5.62	1.57	0.11	0.10
	As_N^{3+}	17.69	4.10	−0.33	5.71	1.47	0.08	0.06
	As_N^{4+}	17.93	3.97	−0.37	5.77	1.41	0.05	
	As_{Ga}^{0}	−3.11	2.13	−1.32	0.38	2.30	1.81	1.84
	As_{Ga}^{1+}	−4.07	2.16	−1.47	0.60	0.45	1.82	1.80

more favorable than Ge_{Al} for doping in AlGaN alloys, conversely to the results of Park and Chadi[26] and the experimental observation.[3] According to previous works for the zinc blende and wurtzite AlN,[22,25,26] Ge_{Al} gives rise to levels very close to the CBM. We calculate a shallow donor level $\varepsilon(1+/0)$ for Ge_{Al}. On the other hand, Ge on a N site requires the first and second neighbors to move outwardly resulting in high relaxation energies. The displacements of the first neighbors induced by Ge_N are similar to the ones for Si_N in AlN. Ge_N induces the deep level $\varepsilon(0/1-)$ and the shallow donor level $\varepsilon(1-/2-)$ in the fundamental gap similar to Si_N. Concerning the stability Ge_N and Si_N present very similar optimal formation energies. For Ge_{Ga} the first and second neighbors experience inward and outward relaxations, respectively. We calculate low formation energies which indicate that Ge would be promptly incorporated on the Ga site under optimal preparation conditions. The shallow donor level $\varepsilon(1+/0)$ corresponding to Ge_{Ga} lies practically at the same energy position as for Si_{Ga}. The first and second neighbors to Ge on the N site experience an outward relaxation in breathing mode. The relaxation and formation energies for Ge_N are higher but comparable with those for Si_N in GaN. The highest ionization level induced by Ge_N in GaN is the deep level $\varepsilon(0/1-)$.

D. Phosphorus

In contrast to the group-IV impurities, P is not expected to introduce any defect level when replacing a N atom in AlN and GaN. Taking into account only the atomic size of P, one may expect that its incorporation is favored on the cation sites. In Table V we present the results for the substitutional P impurity in AlN and GaN. Our calculations show that P on the Al site induces an inward breathing-mode relaxation of the first neighbors and an outward relaxation on the second neighbors. P_{Al} introduce a shallow donor level $\varepsilon(2+/1+)$. P on a N site induces an outward relaxation of the first and second neighbors. Relatively low formation and relaxation energies for P_{Al} are calculated. On the other hand, higher relaxation energies are calculated for P_N accompanied by low optimal formation energies. The highest ionization level $\varepsilon(1+/0)$ associated to P_N in AlN is a deep acceptor level. On the other hand, we also find a shallow donor level $\varepsilon(0/1-)$ for P_N in AlN. According to Mattila and Zunger,[28] the deep level in the case of an isovalent impurity such as P is due to the difference between the size of the atoms and the subsequent difference between the orbital energies of the isovalent atomic species. As far as we know, there is no report about P impurity in *c*-AlN in the literature. In GaN, P_{Ga} forces the first neighbors to displace inwardly and the second neighbors outwardly. P_{Ga} gives rise to the shallow donor

TABLE VII. Displacements of the nearest neighbors 1NN and 2NN ($\Delta\mathbf{d}1,2$ in % of the bond length), lattice relaxation energy ΔE, optimal formation energy for the defect Ω_f (N-rich [cation-rich] for $Sb_{Al,Ga}$ [Sb_N] and *p*-type [*n*-type] for neutral and positively [negatively] ionized), KS defect levels ε_{KS} with respect to the VBM, and ionization levels $\varepsilon(q+1/q)$ for Sb in AlN and GaN.

Impurity		$\Delta\mathbf{d}1$	$\Delta\mathbf{d}2$		ΔE	Ω_f	ε_{KS}	$\varepsilon(q+1/q)$
		$\mathbf{b_{0j}}$	$\mathbf{b_{ij}}$	$\mathbf{n_{ij}}$	(eV)	(eV)	(eV)	(eV)
	Sb_N^{2-}	25.22	7.76	0.24	14.63	5.83	3.19	3.24
	Sb_N^{1-}	24.95	7.77	0.29	14.57	5.88	3.21	3.19
	Sb_N^{0}	24.60	7.79	0.36	14.49	5.98	1.64	1.54
	Sb_N^{1+}	26.72	6.75	0.15	15.70	4.44	1.35	1.26
	Sb_N^{2+}	28.99	5.76	−0.08	16.77	3.18	1.12	1.04
	Sb_N^{3+}	31.41	4.77	−0.29	17.66	2.14	0.96	0.89
	Sb_N^{4+}	33.99	3.75	−0.53	18.43	1.26	0.84	
AlN	Sb_{Al}^{3-}	17.57	3.89	0.19	1.80	3.51	3.20	3.20
	Sb_{Al}^{2-}	17.35	4.01	0.22	1.81	3.61	3.21	3.19
	Sb_{Al}^{1-}	17.05	4.11	0.23	1.83	3.71	3.21	3.16
	Sb_{Al}^{0}	16.54	4.22	0.20	1.85	3.85	2.90	2.95
	Sb_{Al}^{1+}	11.02	4.39	−0.61	1.71	0.90	2.94	2.97
	Sb_{Al}^{2+}	5.41	4.66	−1.40	1.65	−2.07	0.04	0.08
	Sb_{Al}^{3+}	5.40	4.58	−1.38	1.57	−2.15	0.02	0.03
	Sb_{Al}^{4+}	5.39	4.50	−1.36	1.51	−2.18	0.01	
	Sb_N^{0}	20.86	6.62	−0.15	11.25	4.99	0.78	0.75
	Sb_N^{1+}	22.49	5.89	−0.30	11.72	4.24	0.61	0.56
	Sb_N^{2+}	24.13	5.28	−0.46	12.07	3.68	0.48	0.44
	Sb_N^{3+}	25.65	4.72	−0.59	12.32	3.24	0.39	0.35
GaN	Sb_N^{4+}	26.80	4.28	−0.71	12.52	2.88	0.33	
	Sb_{Ga}^{0}	5.57	3.70	−1.02	0.96	2.75	1.74	1.76
	Sb_{Ga}^{1+}	4.27	3.84	−1.23	0.98	0.98	1.73	1.69

level $\varepsilon(2+/1+)$ in the fundamental gap. On the N site, P induces an outward displacement of the first and second neighbors. Higher relaxation energies are expected for P_N in comparison to P_{Ga}, though the formation energies in both cases are low. These results are in excellent agreement with those of Mattila and Zunger[28] for the single P impurity in GaN using the valence force-field method, LDA and 512-atom supercells. The low formation energies calculated show that P_N must be very likely to occur. The KS defect eigenvalues for each charge state follow the ionization levels calculated and the highest level, $\varepsilon(1+/0)$ is in good agreement with those reported in Ref. 28.

E. Arsenic

Previous reports do not study the As impurity in the cubic phase of AlN. As shown in Table VI, As_{Al} presents a very sensitive breathing-mode relaxation with respect to the charge state of the impurity. On the other hand, the relaxation of the second neighbors is outwards and practically not sensitive to the charge state. Due to the similar covalent atomic radii of As and Al, the lattice relaxation energies are small. The optimal formation energies are rather negative for the positively charged states, meaning that As would be promptly incorporated on this Al site for these charge states. We verify that As_{Al} is a negative-*U* center with Hubbard energy $U=-0.1$ eV. Therefore, only the shallow donor level $\varepsilon(1+/0)$ and the shallow acceptor level $\varepsilon(3+/2+)$ are introduced in the fundamental gap by As_{Al}. On the N site, As displaces first and second neighbors outwardly and requires considerable lattice relaxation. A deep acceptor level $\varepsilon(1+/0)$ and a shallow donor level $\varepsilon(0/1-)$ are induced by As_N in AlN. On the Ga site in GaN, As also induces a breathing-mode relaxation of the first neighbors which is inwards, whereas the second-nearest neighbors of As_{Ga} are displaced outwardly. The relaxed geometries with respect to the charge state for As_{Ga} are different from those reported by Van de Walle and Neugebauer in Ref. 30. These differences can be due to the fact that in small supercells the percentage of the total charge variation of the system is higher than for large supercells. The relaxation and formation energies are low for As_{Ga} as well for As_{Al}. As_{Ga} introduces the shallow donor level $\varepsilon(2+/1+)$. On the N site, As displaces the first and second nearest neighbors outwardly, which is in accordance to the results reported by Van de Walle and Neugebauer[30] as well as Mattila and Zunger.[28] The values of the formation energies for As_N are low but higher than for P_N and in between those reported in the Refs. 28 and 30. The KS defect levels agree quantitatively with our calculated ionization levels $\varepsilon(1+/0)$ and $\varepsilon(2+/1+)$, which by their turn agree with the previous calculations.[28,30] However, conversely to the results of Van de Walle and Neugebauer, we do not find that As_N is a negative-*U* center.

F. Antimony

Occupying either the Al or Ga site, Sb is expected to act as double donor. As far as we know, there is no theoretical study on isolated Sb impurities in the literature for cubic AlN and GaN. According to Table VII, Sb gives rise to different effects with respect to the charge state on the Al site in AlN, suggesting that under extreme *p*-type conditions its incorporation is favored. For the charge states with $q<2+$ the outward displacements of the first neighbors are about twice the displacements of the higher positively charged states. Although there are differences in the displacements, the relaxation energies of Sb_{Al} are relatively low. The calculated formation energies suggest that Sb would be promptly incorporated on an Al site for the highest positive charge states. The ionization levels calculated for Sb_{Al} are $\varepsilon(1+/0)$ (donor) and $\varepsilon(3+/2+)$ (acceptor). The level $\varepsilon(2+/1+)$ presents a negative-*U* behavior which means the state $q=1+$ is not stable. On the N site of AlN, Sb requires even larger outward displacements of its nearest neighbors and, as a consequence, the relaxation energies are, the highest among the impurities considered here. The formation energies of Sb_N may vary by 5 eV and decrease with the charge state of the impurity. We derive a shallow donor level $\varepsilon(0/1-)$ and a deep level $\varepsilon(1+/0)$ for Sb_N in AlN. On both Ga and N sites in GaN, Sb displaces the first- and second-nearest neighbors outwardly. The relaxation energies and formation energies for Sb_{Ga} are relatively low. We do not find a

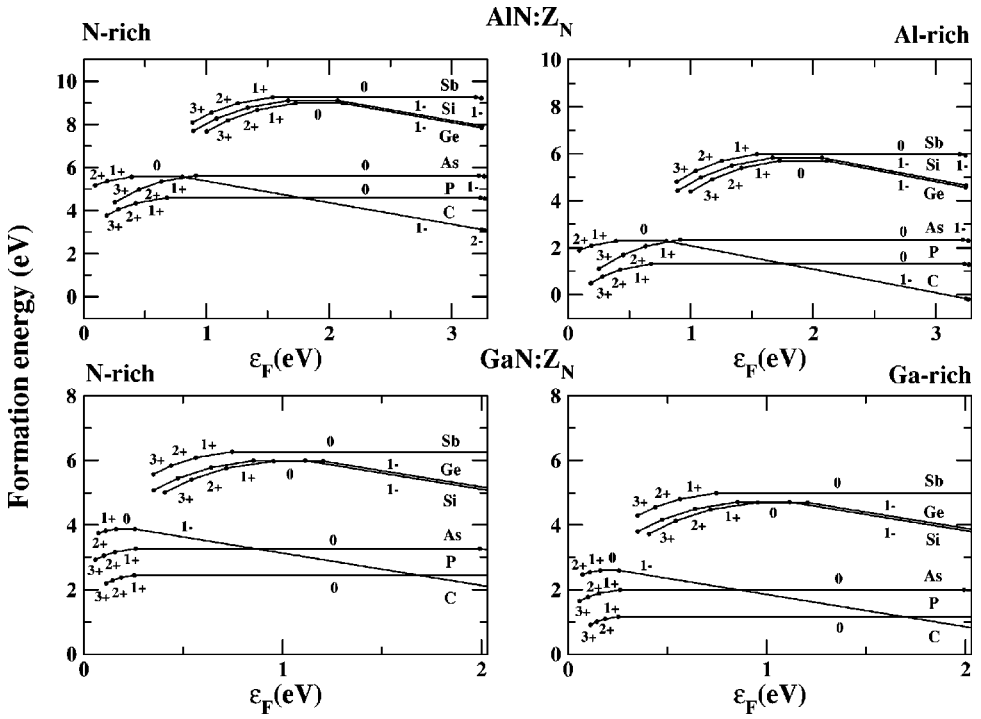

FIG. 1. Formation energies of the impurities $Z=$ C, Si, Ge, P, As, and Sb on the N site of AlN and GaN under N-rich and cation-rich preparation conditions versus reduced Fermi level ε_F. The range of variation of ε_F corresponds to the DFT-LDA fundamental energy gap of AlN (upper panels) and GaN (lower panels).

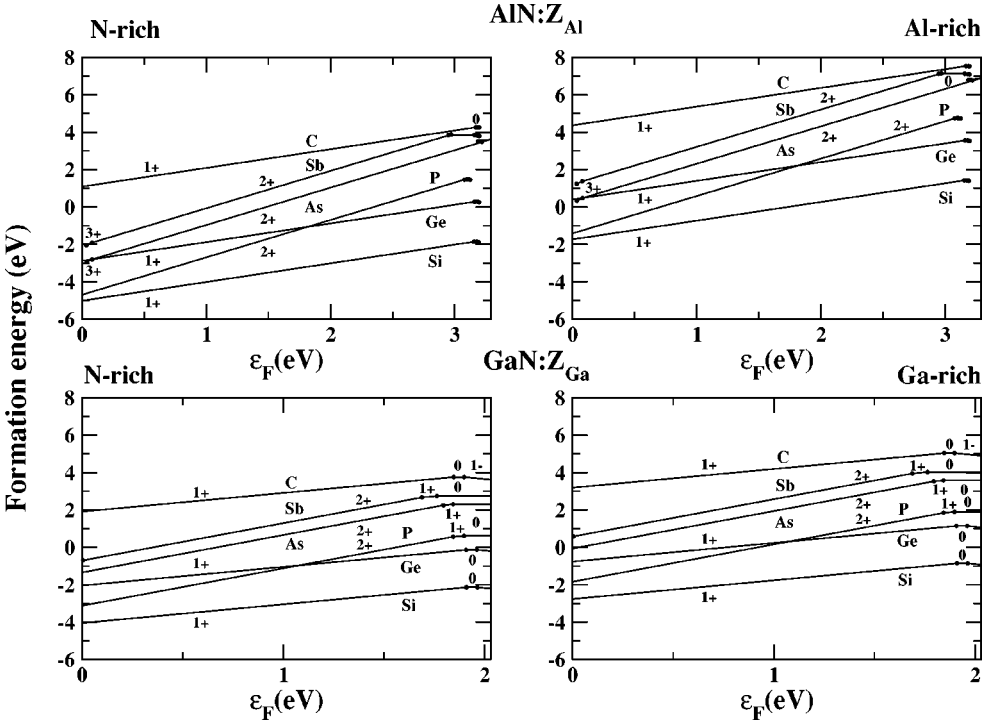

FIG. 2. Formation energies of the impurities $Z=$C, Si, Ge, P, As, and Sb on the cation sites of AlN and GaN under N-rich and cation-rich preparation conditions versus reduced Fermi level ε_F. The range of variation of ε_F corresponds to the DFT-LDA fundamental energy gap of AlN (upper panels) and GaN (lower panels).

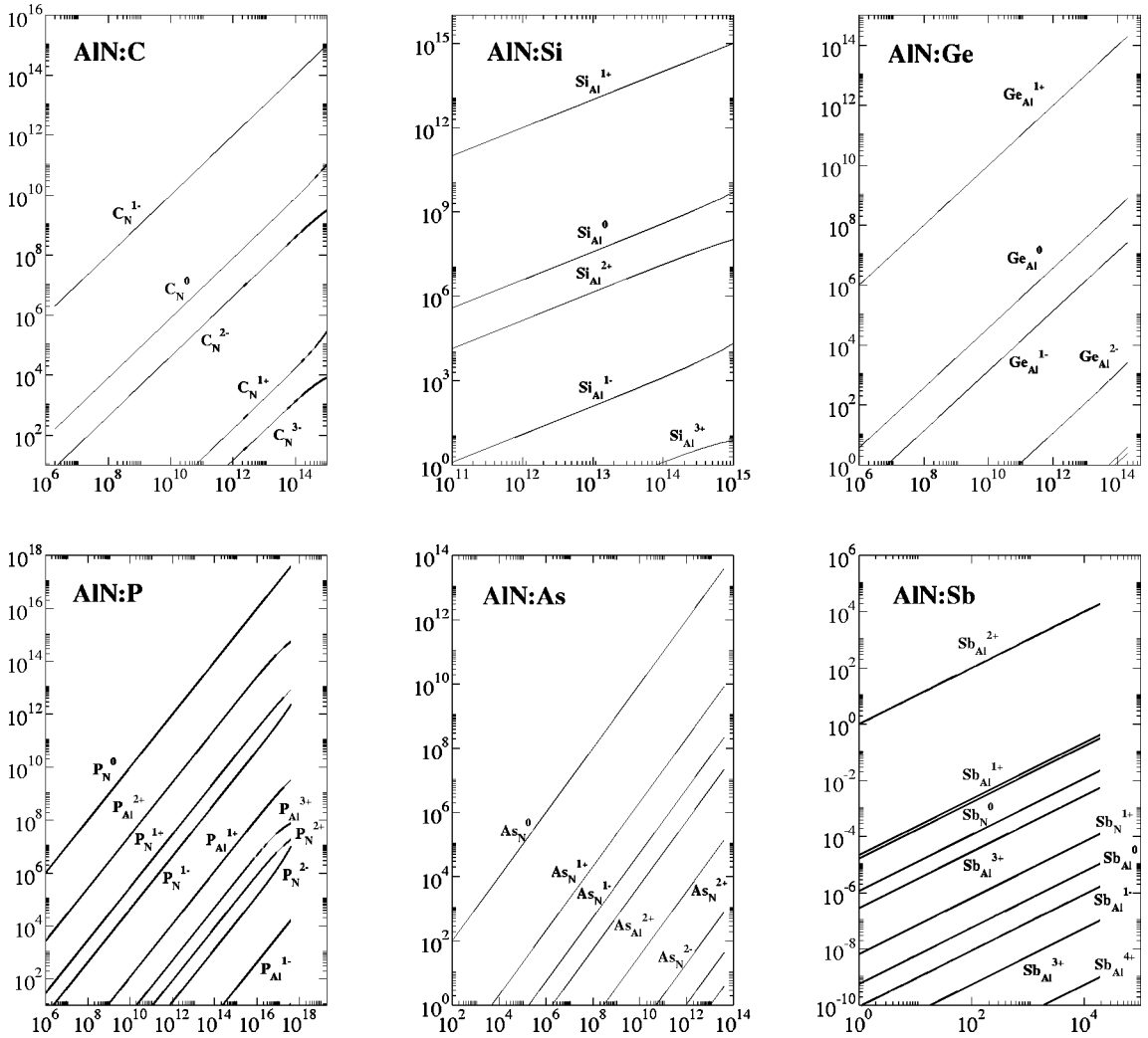

FIG. 3. Calculated partial concentrations (in cm^{-3}) of the substitutional impurity Z=C, Si, Ge, P, As, and Sb in AlN for Al-rich preparation conditions and $T=1300$ K versus total concentration of Z (in cm^{-3}).

negative-U behavior for Sb_{Ga}. The lowest donor level is $\varepsilon(2+/1+)$. Likewise Sb_N in AlN, the relaxation energies of Sb_N in GaN are high. The formation energies for Sb_N decrease with increasing charge of the impurity. We determine the deep acceptor level $\varepsilon(1+/0)$ for Sb_N in GaN.

G. Doping efficiency and impurity concentration

Gaseous nitrogen is one of the least reactive gases in the nature due to the strong triple bonds between the atoms. In the N_2 molecule the strong bonds result in a very high cohesive energy ($E_{coh}=9.8$ eV). As a consequence, when it is used as a source for nitrogen atomic species, high dissociation energies are required and those cannot be achieved under usual growth conditions except in plasma growth environment.[52] During the growth of GaN, Ga-rich preparation conditions give rise to growing surfaces with better morphology and high mobility for the atoms.[53] However, the initial growth conditions needed for the nucleation of cubic GaN require a N/Ga flux ratio higher than 1 for temperatures lower than 1050 K.[54] For higher temperatures, Ga-rich preparation conditions favors the nucleation of cubic GaN. Under these preparation conditions, the incorporation of impurities is likely to occur on the nitrogen site. In Fig. 1 we show the formation energies of the C, Si, Ge, P, As, and Sb impurities substitutional on N site in AlN and GaN for several preparation conditions. As a rule, the incorporation of the six impurities on this site under fixed preparation conditions is more favorable in GaN than in AlN. Carbon, phosphorus and arsenic have lower formation energy than germanium, silicon, and antimony in both AlN and GaN. Sb, Si, and Ge give rise to relatively deep acceptor levels, whereas C, P, and As produce shallow acceptor levels. The formation energies of the impurities on cation sites are shown in Fig. 2 for N-rich and cation-rich preparation conditions, and versus the reduced Fermi level ε_F. Taking into account the trend of the formation energies one verifies that on cation sites Si, Ge, and P are more favored energetically than the other impurities. For wide range of ε_F, the group-IV impurities prefer the charge state $q=1+$, whereas the group-V impurities are in the charge state $q=2+$, i.e., the charge state that makes the impurity isoelectronic to the corresponding site in the

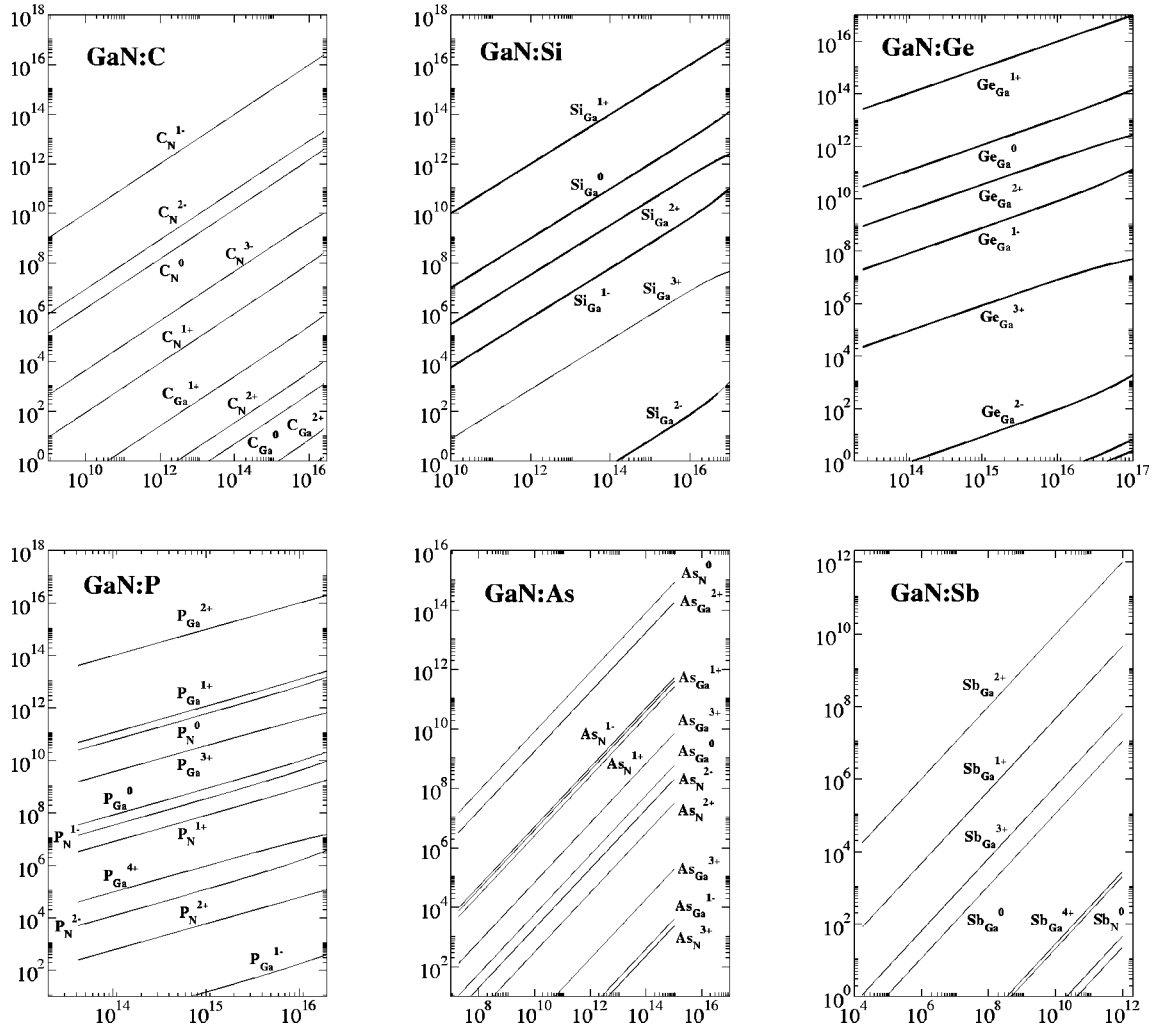

FIG. 4. Calculated partial concentrations (in cm^{-3}) of the substitutional impurity Z=C, Si, Ge, P, As, and Sb in GaN for Ga-rich preparation conditions and $T=1300$ K versus total concentration of Z (in cm^{-3}).

host crystal. Carbon and antimony are the least favored impurities on cation sites and silicon is the most favored impurity taking into account the trend of the values for the formation energies. Negative formation energies are unphysical if one considers the calculated partial concentration of impurities $C[Z]=N_S\exp[S_f/k_B-\Omega_f/(k_BT)]$ in the total concentration of substitutional sites $N_S=4/(\text{lattice constant})^3$. However, taking into account the entropy of impurity formation S_f one should obtain the correct formation energies. Since Sb has high formation energies for both nitrogen and cation sites, we confirm its use in many growth experiments as a surfactant for both AlN and GaN.[16,17]

Studying each of the six impurities Z separately and its charge states q as well as the charge neutrality condition involving hole (p) and electron (n) concentrations

$$\sum_i q_i C[Z^{q^i}]+p-n=0, \tag{1}$$

one determines the Fermi level ε_F for which the crystal fulfils the charge-neutrality condition. The partial concentrations of the substitutional defects Z with charge q are plotted versus the total concentration of the impurity $C[Z]^{\text{total}}=N_S\Sigma_i\exp[S_f^i/k_B-\Omega_f^i/(k_BT)]$ in Figs. 3 and 4 for cation-rich preparation conditions and for a growth temperature $T=1300$ K. The total concentration of Z is controlled by decreasing the chemical potential $\mu(Z)$ towards negative values and $\mu(Z)=\mu(Z_{\text{bulk}})$ correspond to the maximum concentration of Z. The entropy of formation S_f^i is set equal to zero for each charge state i of a given impurity Z in our approximation. To calculate the hole and electron concentrations we apply the corresponding values of the effective masses reported in Ref. 55. The effective masses for holes are averaged among their values in three directions. We have to mention that the results in Figs. 3 and 4 can be drastically changed if additional defects are considered in Eq. (1). Altogether, there is a tendency for the underestimation of the evaluated concentrations.

The concentrations calculated for AlN in Fig. 3 show that the highest incorporation occurs for the impurities in their neutral and isoelectronic charge states. Carbon, phosphorus and arsenic are incorporated mainly on the nitrogen site, whereas silicon, germanium, and antimony are incorporated

in higher concentration on the aluminum site. According to the calculations, carbon, phosphorus, and arsenic are incorporated in concentrations varying from 10^{13}–10^{18} cm^{-3}, whereas antimony will be incorporated in negligible concentrations from the experimental point of view. Phosphorus appears as the impurity with the highest concentration (10^{18} cm^{-3}) in cubic AlN. In Fig. 4 the calculated concentrations of the impurities in GaN are plotted. Except for P, the concentration of the other impurities follows in general the trend observed in AlN. Phosphorus, in principle, would prefer to lose two electrons to be incorporated on the gallium site. In the thermodynamic equilibrium the concentrations of silicon and germanium should be 10^{2}–10^{3} cm^{-3} higher in GaN than in AlN. Antimony should be incorporated in negligible concentrations for both AlN and GaN. According to our calculations, carbon and arsenic concentrations are slightly lower in GaN than those calculated for AlN. In particular for carbon, the concentration of $10^{15}-10^{16}$ cm^{-3} is similar to the one reported in Ref. 10 by Köhler and coworkers for the concentration of holes in *c*-GaN (6×10^{17} cm^{-3}) due to the intentional doping with carbon. Although our calculated concentrations must be interpreted qualitatively, the concentration measured by Guido *et al.*[19] and Li *et al.*[20] for growth temperatures of about 1300 K in *w*-GaN agree within two or three orders of magnitude. In the study of Kuroiwa and co-workers for the $GaN_{1-x}P_x$ and $GaN_{1-x}As_x$ alloys, maximum compositions x of 0.37% (1.7×10^{18} cm^{-3}) and 0.26% (1.2×10^{18} cm^{-3}), respectively, deviate only by 10^{2} to 10^{3} cm^{-3}.

IV. SUMMARY

In this paper we presented a comprehensive study of group-IV and group-V substitutional impurities in cubic AlN and GaN, concerning to the relaxed geometry of the nearest neighbors, energetical stability, defect levels, and partial concentrations incorporated according to the charge state of the impurity. In comparison to previous studies, we attenuated the alloying effect and the impurity-impurity interaction resulting from the use of the supercell approximation. In general, the impurities on the nitrogen site give rise to well-defined acceptor levels, whereas the incorporation of impurities on the cation sites leads to shallow donor levels. On the N site we found that C, P, and As are the most stable impurities introducing mainly shallow acceptor levels. On the other hand, Si, Ge, and P are the most stable impurities on the cation sites for both AlN and GaN. Antimony possesses high formation energies for both substitutional sites and nitrides considered, which confirms its use as a surfactant. For a large range of the Fermi levels the charge state of the impurity is the one which makes it isoelectronic on the site of the host crystal. In general, there is a good agreement between the KS impurity levels and the ionization levels calculated by means of the ΔSCF method. Although the approximations used (e.g., the neglected entropy effects) for the concentration of impurities correspond to a more qualitative analysis, we found agreement with respect to the trends, in particular with the charge state. The absolute values for the concentrations are in general two or three orders of magnitude smaller than the experimental values. Also the highest partial concentrations refer to the charge states for which the impurity is isoelectronic to the replaced atom in the host crystal.

ACKNOWLEDGMENTS

This work was supported by the Deutsche Forschungsgemeinschaft in the framework of the central project ''Group-III nitrides and their heterostructures: Growth, basic properties and applications'' (Grant No. Be 1346/8-5) and the Brazilian funding agencies FAPESP and CNPq.

[1] J.H. Edgar, *Properties of Group-III Nitrides* (INSPEC, London, 1994).
[2] H. Okumura, H. Hamaguchi, K. Ohta, G. Feuillet, K. Balakrishnan, Y. Ishida, S. Chichibu, H. Nakanishi, T. Nagatomo, and S. Yoshida, Mater. Sci. Forum **264**, 1167 (1998).
[3] X. Zhang, P. Kung, A. Saxler, D. Walker, T.C. Wang, and M. Razeghi, Appl. Phys. Lett. **67**, 1745 (1995).
[4] L.B. Rowland, K. Doverspike, and D.K. Gaskill, Appl. Phys. Lett. **66**, 1495 (1995).
[5] W. Götz, N.M. Johnson, C. Chen, H. Liu, C. Kuo, and W. Imler, Appl. Phys. Lett. **68**, 3144 (1996).
[6] S.T.B. Goennenwein, R. Zeisel, O. Ambacher, M.S. Brandt, M. Stutzmann, and S. Baldovino, Appl. Phys. Lett. **79**, 2396 (2001).
[7] D.J. As, T. Simonsmeier, J. Busch, B. Schöttker, M. Lübbers, J. Mimkes, D. Schikora, K. Lischka, W. Kriegseis, W. Burkhardt, and B.K. Meyer, MRS Internet J. Nitride Semicond. Res. **4S1**, G 3.24 (1999).
[8] D.J. As and U. Köhler, J. Phys.: Condens. Matter **13**, 8923 (2001).
[9] C.R. Abernathy, J.D. MacKenzie, and S.J. Pearton, Appl. Phys. Lett. **66**, 1969 (1995).
[10] U. Köhler, M. Lübbers, J. Mimkes, and D.J. As, Physica B **308-310**, 126 (2001).
[11] M.P. Thompson, G.W. Auner, T.S. Zheleva, K.A. Jones, S.J. Simko, and J.N. Hilfiker, J. Appl. Phys. **89**, 3331 (2001).
[12] S. Fischer, C. Wetzel, E.E. Haller, and B.K. Meyer, Appl. Phys. Lett. **67**, 1298 (1995).
[13] G.-C. Yi and B.W. Wessels, Appl. Phys. Lett. **70**, 357 (1997).
[14] X. Tang, F. Hossain, K. Wongchotigul, and M.G. Spencer, Appl. Phys. Lett. **72**, 1501 (1998).
[15] Y. Zhao, C.W. Tu, I.-T. Bae, and T.Y. Seong, Appl. Phys. Lett. **74**, 3182 (1999).
[16] L. Zhang, H.F. Tang, and T.F. Kuech, Appl. Phys. Lett. **79**, 3059 (2001).
[17] M. Copel, M.C. Reuter, M. Horn von Hoegen, and R.M. Tromp, Phys. Rev. B **42**, 11 682 (1990).
[18] J.I. Pankove and J.A. Hutchby, J. Appl. Phys. **47**, 5387 (1976).
[19] L.J. Guido, P. Mitev, M. Gherasimova, and B. Gaffey, Appl. Phys. Lett. **72**, 2005 (1998).

[20] X. Li, S. Kim, E.E. Reuter, S.G. Bishop, and J.J. Coleman, Appl. Phys. Lett. **72**, 1990 (1998).
[21] R. Kuroiwa, H. Asahi, K. Asami, S.-J. Kim, K. Iwata, and S. Gonda, Appl. Phys. Lett. **73**, 2630 (1998).
[22] D.W. Jenkins and J.D. Dow, Phys. Rev. B **39**, 3317 (1989).
[23] J. Neugebauer and C.G. Van de Walle, Adv. Solid State Phys. **35**, 25 (1996).
[24] C.G. Van de Walle, J. Neugebauer, C. Stampfl, M.D. McCluskey, and N.M. Johnson, Acta Phys. Pol. A **96**, 613 (1999).
[25] P. Bogusławski and J. Bernholc, Phys. Rev. B **56**, 9496 (1997).
[26] C.H. Park and D.J. Chadi, Phys. Rev. B **55**, 12 995 (1997).
[27] I. Gorczyca, A. Svane, and N.E. Christensen, Solid State Commun. **101**, 747 (1997).
[28] T. Mattila and A. Zunger, Phys. Rev. B **58**, 1367 (1998).
[29] T. Mattila and A. Zunger, Phys. Rev. B **59**, 9943 (1999).
[30] C.G. Van de Walle and J. Neugebauer, Appl. Phys. Lett. **76**, 1009 (2000).
[31] R. Enderlein and N.J. Horing, *Fundamentals of Semiconductor Physics and Devices* (World Scientific, Singapore 1997).
[32] P. Hohenberg and W. Kohn, Phys. Rev. **136**, B864 (1964).
[33] W. Kohn and L.J. Sham, Phys. Rev. **140**, A1139 (1965).
[34] J.P. Perdew and A. Zunger, Phys. Rev. B **23**, 5048 (1981).
[35] D.M. Ceperley and B.J. Alder, Phys. Rev. Lett. **45**, 566 (1980).
[36] D. Vanderbilt, Phys. Rev. B **41**, 7892 (1990).
[37] G. Kresse and J. Furthmüller, Comput. Mater. Sci. **6**, 15 (1996).
[38] L.E. Ramos, J. Furthmüller, L.M.R. Scolfaro, J.R. Leite, and F. Bechstedt, Phys. Rev. B **66**, 075209 (2002).
[39] M. Methfessel and A.T. Paxton, Phys. Rev. B **40**, 3616 (1989).
[40] K. Laasonen, R.M. Nieminen, and M.J. Puska, Phys. Rev. B **45**, 4122 (1992).
[41] S. Pöykkö, M.J. Puska, and R.M. Nieminen, Phys. Rev. B **53**, 3813 (1996).
[42] H.B. Callen, *Thermodynamics and an Introduction to Thermostatistics*, 2nd ed. (Wiley, Singapore 1985).
[43] G. Harbeke, O. Madelung, and U. Rössler, in *Numerical Data and Functional Relationships in Science and Technology*, Landoldt-Börnstein New Series Group III, Vol. 17 (Springer-Verlag, Berlin 1982).
[44] K.J. Chang and M.L. Cohen, Phys. Rev. B **33**, 6177 (1986); **33**, 7371 (1986).
[45] T. Kikegawa and H. Iwasaki, Acta Crystallogr., Sect. B: Struct. Sci. **39**, 158 (1983).
[46] X. Gonze, J.-P. Michenaud, and J.-P. Vigneron, Phys. Rev. B **41**, 11 827 (1990).
[47] U. Großner, J. Furthmüller, and F. Bechstedt, Appl. Phys. Lett. **74**, 3851 (1999).
[48] L. Torpo, R.M. Nieminen, K.E. Laasonen, and S. Pöykkö, Appl. Phys. Lett. **74**, 221 (1999).
[49] A. Zywietz, J. Furthmüller, and F. Bechstedt, Phys. Rev. B **59**, 15 166 (1999).
[50] G.A. Baraff and M. Schlüter, Phys. Rev. B **30**, 1853 (1984).
[51] C. Kittel, *Introduction to Solid State Physics* (Wiley, New York 1966).
[52] H. Morkoç, J. Mater. Sci.: Mater. Electron. **12**, 677 (2001).
[53] B. Heying, R. Averbeck, L.F. Chen, E. Haus, H. Riechert, and J.S. Speck, J. Appl. Phys. **88**, 1855 (2000).
[54] D. Schikora, M. Hankeln, D.J. As, K. Lischka, T. Litz, A. Waag, T. Buhrow, and F. Henneberger, Phys. Rev. B **54**, R8381 (1996).
[55] L.E. Ramos, L.K. Teles, L.M.R. Scolfaro, J.L.P. Castineira, A.L. Rosa, and J.R. Leite, Phys. Rev. B **63**, 165210 (2001).